

# ShOpt.jl | A Julia Library for Empirical Point Spread Function Characterization of JWST NIRCам Data

Edward Berman<sup>1</sup> and Jacqueline McCleary<sup>1</sup>

<sup>1</sup> Northeastern University, USA ¶ Corresponding author

DOI: [10.xxxxxx/draft](https://doi.org/10.xxxxxx/draft)

## Software

- [Review](#)
- [Repository](#)
- [Archive](#)

Editor: [Open Journals](#)

## Reviewers:

- [@openjournals](#)

Submitted: 01 January 1970

Published: unpublished

## License

Authors of papers retain copyright and release the work under a Creative Commons Attribution 4.0 International License ([CC BY 4.0](#))

## In partnership with



This article and software are linked with research article DOI [10.3847/xxxxx](https://doi.org/10.3847/xxxxx), published in the Astronomical Journal.

## Summary

## Introduction

When astronomers take pictures of space, optical properties of the camera and atmospheric effects distort the incoming light. Stars are examples of what astronomers call point sources. Before any distortion is applied to an image, point sources of light can be thought of as delta functions. The aptly named point spread function (PSF) is a mathematical model that quantifies exactly how the light is being distorted. The point spread function takes as input a delta function and a position and outputs a distorted image. It can be thought of as the impulse response of an optical system to incoming light. The goal of point spread function characterization is to be able to point to any position on your camera and predict what the distortion looks like. Once we have a model that can do this well, we can deconvolve our images with the point spread function to obtain what the image would look like in the absence of distortion. The empirical way to do this is to take our image and generate a catalog of all of the distorted stars inside of it. Then, we separate the catalog into training and validation sets. Our PSF will be found by interpolating the training stars across the field of view of the camera. After training, our PSF is validated by comparing the reserved stars to the PSF model's prediction.

Shear Optimization with ShOpt.jl introduces modern techniques for empirical point spread function characterization across the field of view tailored to the data captured by the James Webb Space Telescope (JWST). We can approximate our stars with analytic profiles. This gives us a rough idea of the size and shape of the point spread function and doubles as a mechanism to clean data. We adopt a multivariate gaussian profile because it is computationally cheap to fit to an image. That is, it is easy to differentiate and doesn't involve any numeric integration or other costly steps to calculate. Other common fits such as Kolmogorov fits involve numeric integration and thus take much longer to fit. The JWST point spread functions are very "spikey" as seen below, and as a result, analytic profiles are limited in their ability to model the point spread function. Thus, the usual advantages of a more expensive analytic profile are mute.

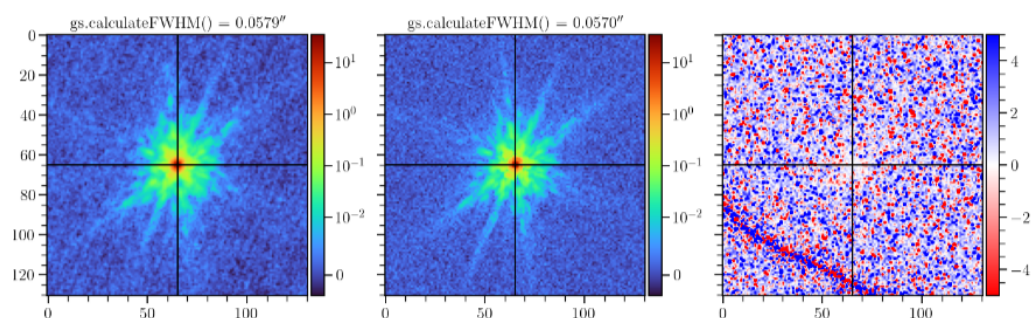


**Figure 1:** The plot on the left represents the average cutout of all of the stars in a supplied catalog. Likewise, plot in the middle represents the average point spread function model. The plot on the right represents the average normalized error between the observed star cutouts and the point spread function model

Our multivariate gaussian is parameterized by three variables,  $[s, g_1, g_2]$ , where  $s$  corresponds to size and  $g_1, g_2$  correspond to shear. A shear matrix has the form

$$\begin{pmatrix} 1 + g_1 & g_2 \\ g_2 & 1 - g_1 \end{pmatrix}$$

35 . Given a point  $[u, v]$ , we obtain coordinates  $[u', v']$  by applying a shear and then a scaling  
 36 by  $\frac{s}{\sqrt{1-g_1^2-g_2^2}}$ . Then, we choose  $f(r) := Ae^{-r^2}$  to complete our fit, where  $A$  makes the fit  
 37 sum to unity over the cutout of our star. After we fit this function to our stars with `Optim.jl`  
 38 ([Mogensen & Riseth, 2018](#)) and `ForwardDiff.jl` ([Revels et al., 2016](#)), we interpolate the  
 39 parameters across the field of view according to position. Essentially, each star is a datapoint,  
 40 and the three variables are treated as polynomials in focal plane coordinates of degree  $n$ , where  
 41  $n$  is supplied by the user. The focal plain refers to the set of points where an image appears to  
 42 be in perfect focus. This is instead of pixel coordinates, where one just uses  $(x, y)$  as measured  
 43 on an image. For a more precise model, we also give each pixel in our star stamp a polynomial  
 44 and interpolate it across the field of view. That is, each pixel in position  $(i, j)$  of a star cutout  
 45 gets its own polynomial, interpolated over  $k$  different star cutouts at different locations in the  
 46 focal plane. This is referred to in the literature as a pixel basis ([Jarvis et al., 2020](#)).

## 47 Notation

48 1. For the set  $B_2(r)$ , we have:

$$B_\circ(r) \equiv \{[x, y] : x^2 + y^2 < 1\} \subset \mathbb{R}^2$$

49 2. For the set  $\mathbb{R}_+$ , we have:

$$\mathbb{R}_+ \equiv \{x : x > 0\} \subset \mathbb{R}$$

50 3. For the Cartesian product of sets  $A$  and  $B$ , we have:

$$A \times B \equiv \{(a, b) : a \in A, b \in B\}$$

## 51 Methods

Sh0pt.jl takes inspiration from a number of algorithms outside of astronomy. Mainly, SE-Sync (Rosen et al., 2019), an algorithm that provides a certifiably correct solution to a robotic mapping problem by considering the manifold properties of the data. SE-Sync proves that with

55 sufficiently clean data, their algorithm will descend to a global minimum constrained to the  
 56 manifold  $SE(d)^n/SE(d)$ . Likewise, we are able to put a constraint on the solutions we obtain  
 57 to  $[s, g_1, g_2]$  to a manifold. The solution space to  $[s, g_1, g_2]$  is constrained to the manifold  
 58  $B_2(r) \times \mathbb{R}_+$  (Bernstein & Jarvis, 2002). While it was known that this constrain existed in  
 59 the literature, the parameter estimation task is generally framed as an unconstrained problem  
 60 (Jarvis et al., 2020). For a more rigorous treatment of optimization on manifolds see (Absil  
 61 et al., 2008) and (Boumal, 2023). Julia has lots of support for working with manifolds with  
 62 Manopt, which we may leverage in future releases (Bergmann, 2022).

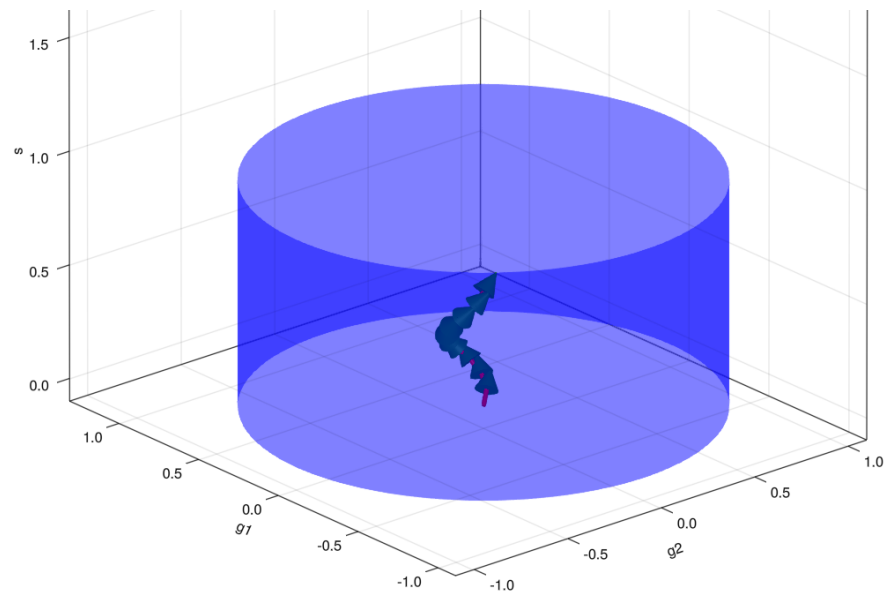


**Figure 2:** LFBGS algorithm used to find parameters subject to the cylindrical constraint.  $s$  is arbitrarily capped at 1 as a data cleaning method.

63 ShOpt.jl provides two modes for pixel grid fits, PCA mode and Autoencoder mode. PCA mode,  
 64 outlined below, reconstructs its images using the first  $n$  principal components. Autoencoder  
 65 mode uses a neural network to reconstruct the image from a lower dimensional latent space.  
 66 The network code written with Flux.jl is also outlined below (Innes, 2018). Both modes  
 67 provide the end user with tunable parameters that allow for both perfect reconstruction of  
 68 star cutouts and low dimensional representations. The advantage of these modes is that they  
 69 provide good reconstructions of the distorted images that can learn the key features of the  
 70 point spread function without overfitting the background noise. In this way it generates a  
 71 datapoint for our algorithm to train on and denoises the image in one step.

72 PCA mode

```
function pca_image(image, ncomponents)
    #Load img Matrix
    img_matrix = image

    # Perform PCA
    M = fit(PCA, img_matrix; maxoutdim=ncomponents)

    # Transform the image into the PCA space
    transformed = MultivariateStats.transform(M, img_matrix)

    # Reconstruct the image
    reconstructed = reconstruct(M, transformed)
```

```

# Reshape the image back to its original shape
reconstructed_image = reshape(reconstructed, size(img_matrix)...)
end

73 Autoencoder mode

# Encoder
encoder = Chain(
    Dense(r*c, 128, leakyrelu),
    Dense(128, 64, leakyrelu),
    Dense(64, 32, leakyrelu),
)

#Decoder
decoder = Chain(
    Dense(32, 64, leakyrelu),
    Dense(64, 128, leakyrelu),
    Dense(128, r*c, tanh),
)

#Full autoencoder
autoencoder = Chain(encoder, decoder)

#x_hat = autoencoder(x)
loss(x) = mse(autoencoder(x), x)

# Define the optimizer
optimizer = ADAM()

```

## 74 Statement of need

75 We can trace the first empirical PSF fitters back to DAOPHOT (Stetson, 1987). PSFex made  
76 major advancements in precise PSF modeling. With PSFex, you could interpolate several  
77 different bases, including a basis of pixels, instead of relying on simple parametric functions.  
78 PSFex was built as a general purpose tool and to this day is widely used. Newer empirical  
79 PSF fitters are geared toward large scale surveys and the difficulties that arise specific to  
80 those datasets. As an example, The Dark Energy Survey and DESCam (Flaugher et al., 2015;  
81 Jarvis et al., 2020) sparked the creation of PIFF. The recent data from the James Webb Space  
82 Telescope poses new challenges.

- 83 (1) The JWST PSFs are not well approximated by analytic profiles as seen in Figure 1. This  
84 calls for well thought out parametric free models that can capture the full dynamic range  
85 of the Point Spread Function without fixating on the noise in the background. Previously,  
86 Rowe statistics and other parametric equations were used to diagnose PSF accuracy  
87 (Rowe, 2010). ShOpt provides a suite of parametric free summary statistics out of the  
88 box.
- 89 (2) The NIRCcam detectors are 0.03"/pix or 0.06" /pix (Beichman et al., 2012a; Rieke et al.,  
90 2003, 2005). To capture an accurate description of the point spread function at this  
91 scale we need images that are 131 by 131 to 261 by 261 pixels across. These vignet  
92 sizes are much larger in comparison to the sizes needed for previous large surveys such  
93 as DES (Jarvis et al., 2020) and SuperBIT (McCleary et al., 2023) and forces us to  
94 evaluate how well existing PSF fitters scale to this size. The DES and SuperBIT surveys  
95 needed PSF sizes of 17 by 17 and 48 by 48, an order of magnitude less than the JWST  
96 PSF sizes.

## 97 State of the Field

98 There are several existing empirical PSF fitters in addition to a forward model of the JWST  
99 PSFs developed by STScI (Jarvis et al., 2020 ; Bertin, 2011; Perrin et al., 2014 ; Perrin et  
100 al., 2012). We describe them here and draw attention to their strengths and weaknesses to  
101 motivate the development of ShOpt.jl. As described in the statement of need, PSFex was one  
102 of the first precise and general purpose tools used for empirical PSF fitting. However, PSFex  
103 produced a systematic size bias of the point spread function with how it calculated spatial  
104 variation across the field of view (Jarvis et al., 2020). It was discovered via the analytic profile  
105 fits that the size of the point spread function, governed by the variable  $[s]$ , was underestimated.

106 PIFF (Point Spread Functions in the Full Field of View) followed PSFex in the effort to correct  
107 this issue. The DES camera was 2.2 degrees across, which was large enough for the size bias  
108 to become noticable for their efforts. PIFF works in focal plane coordinates as opposed to sky  
109 coordinates which fixes the systematic size bias. Jarvis and DES also used the Python libraries  
110 of astropy (Astropy Collaboration et al., 2022) and Galsim (Rowe et al., 2015) to make the  
111 software more accessible than PSFex to programmers in the astrophysics community. PSFex  
112 was written in C and has been active for more than 20 years. Due to being so old and written  
113 in a low level language it is much less approachable for a community of open source developers.  
114 One of the motivations of ShOpt was to write astrophysics specific software in Julia, because  
115 Julia provides a nice balance of readability and speed with it's high level functional paradigm  
116 and just in time compiler.

117 While we do have forwards models of the JWST PSF, these models are for single exposure  
118 images. The JWST images are either single exposure or mosaics (Perrin et al., 2014, 2012).  
119 Mosaiced images are essentially single exposure detector images averaged together. To account  
120 for the rotation of the camera between the capture of images and the wide field of view,  
121 there are a number of steps that make applying these forward models to mosaics a non trivial  
122 procedure.

123 The COMOS-Web survey is the largest JWST extragalactic survey according to area and  
124 prime time allocation (Casey et al., 2023), and takes up  $0.54 \text{ deg}^2$  (Beichman et al., 2012b;  
125 Rieke et al., 2023). This is a large enough portion of the sky that we should prepare to see a  
126 lot of variation across the field of view. This gives ShOpt the opportunity to validate PIFF's  
127 correction for handling PSF variations and test how impactful (or not impactful) PSFex's size  
128 bias is.

## 129 Future Work

130 We speculate that petal diagrams may be able to approximate the spikey natures of JWST  
131 PSFS. Consider  $r = A \cos(k\theta + \gamma)$ , shown below in figure 3 for different  $[A, k]$  values where  
132  $\gamma = 0$ . In practice,  $[A, k, \gamma]$  could be learnable parameters. We could then choose some  
133  $f(r) \propto \frac{1}{r}$  such that the gray fades from black to white. We would define  $f(r)$  piece wise such  
134 that it is 0 outside of the petal and decreases radially with  $r$  inside the petal.

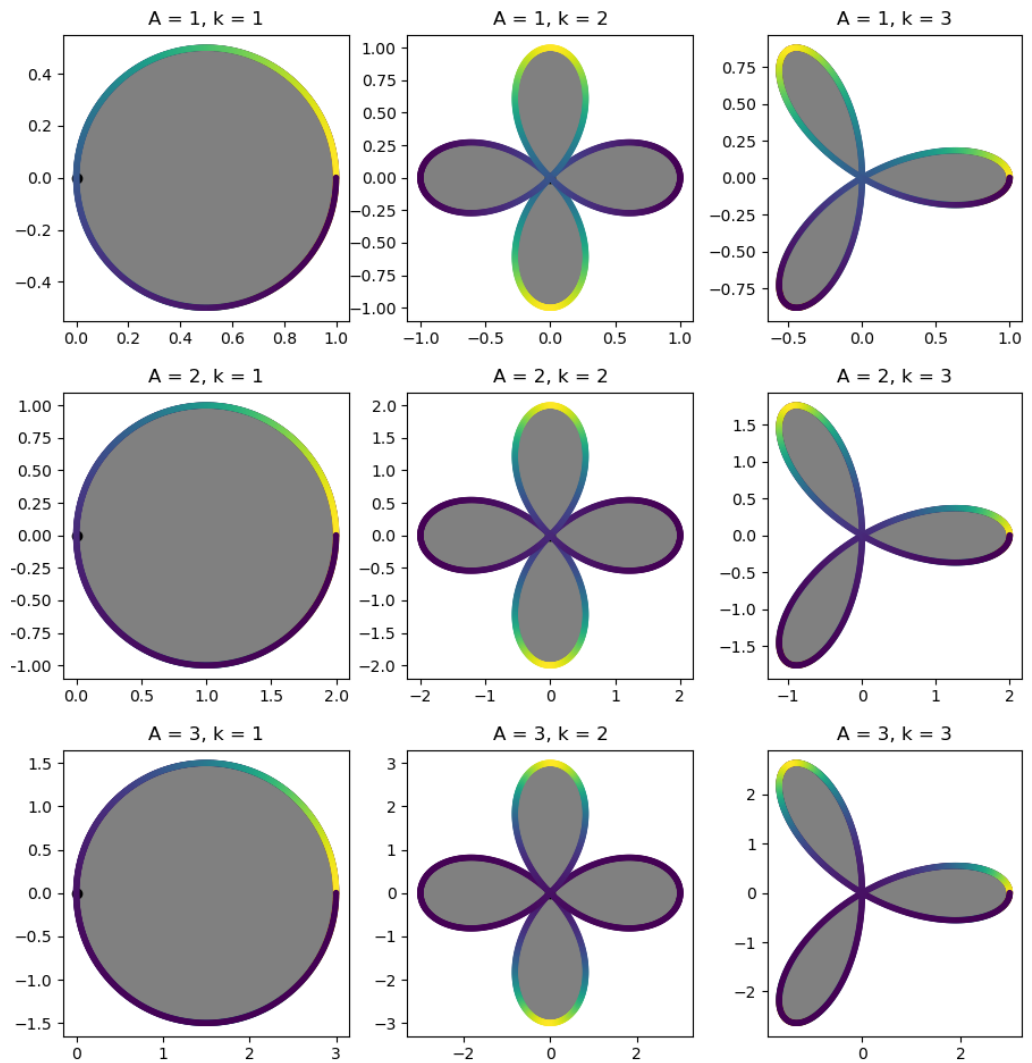


Figure 3: Petal Diagram

## Acknowledgements

This material is based upon work supported by a Northeastern University Undergraduate Research and Fellowships PEAK Experiences Award. We would also like to thank the Northeastern Physics Department for making this project possible through the Physics Co-op Research Fellowship. Support for this work was provided by NASA through grant JWST-GO-01727 and HST-AR- 15802 awarded by the Space Telescope Science Institute, which is operated by the Association of Universities for Research in Astronomy, Inc., under NASA contract NAS 5-26555. This work was made possible by utilizing the CANDIDE cluster at the Institut d'Astrophysique de Paris. Finally, we would like to thank Northeastern Research Computing for access to their servers. Additionally, we'd like to extend a thank you to Professor David Rosen for giving some valuable insights during the early stages of this work.



## References

- Absil, P.-A., Mahony, R., & Sepulchre, R. (2008). *Optimization algorithms on matrix manifolds* (p. xvi+224). Princeton University Press. ISBN: 978-0-691-13298-3
- Astropy Collaboration, Price-Whelan, A. M., Lim, P. L., Earl, N., Starkman, N., Bradley, L., Shupe, D. L., Patil, A. A., Corrales, L., Brasseur, C. E., Nöthe, M., Donath, A., Tollerud, E., Morris, B. M., Ginsburg, A., Vaher, E., Weaver, B. A., Tocknell, J., Jamieson, W., ... Astropy Project Contributors. (2022). The Astropy Project: Sustaining and Growing a Community-oriented Open-source Project and the Latest Major Release (v5.0) of the Core Package. *935*(2), 167. <https://doi.org/10.3847/1538-4357/ac7c74>
- Beichman, C. A., Rieke, M., Eisenstein, D., Greene, T. P., Krist, J., McCarthy, D., Meyer, M., & Stansberry, J. (2012b). Science opportunities with the near-IR camera (NIRCam) on the James Webb Space Telescope (JWST). In M. C. Clampin, G. G. Fazio, H. A. MacEwen, & J. M. O. Jr. (Eds.), *Space telescopes and instrumentation 2012: Optical, infrared, and millimeter wave* (Vol. 8442, p. 84422N). International Society for Optics; Photonics; SPIE. <https://doi.org/10.1117/12.925447>
- Beichman, C. A., Rieke, M., Eisenstein, D., Greene, T. P., Krist, J., McCarthy, D., Meyer, M., & Stansberry, J. (2012a). Science opportunities with the near-IR camera (NIRCam) on the James Webb Space Telescope (JWST). In M. C. Clampin, G. G. Fazio, H. A. MacEwen, & Jr. Oschmann Jacobus M. (Eds.), *Space telescopes and instrumentation 2012: Optical, infrared, and millimeter wave* (Vol. 8442, p. 84422N). <https://doi.org/10.1117/12.925447>
- Bergmann, R. (2022). Manopt.jl: Optimization on manifolds in Julia. *Journal of Open Source Software*, *7*(70), 3866. <https://doi.org/10.21105/joss.03866>
- Bernstein, G. M., & Jarvis, M. (2002). Shapes and shears, stars and smears: Optimal measurements for weak lensing. *The Astronomical Journal*, *123*(2), 583. <https://doi.org/10.1086/338085>
- Bertin, E. (2011). Automated Morphometry with SExtractor and PSFEx. In I. N. Evans, A. Accomazzi, D. J. Mink, & A. H. Rots (Eds.), *Astronomical data analysis software and systems XX* (Vol. 442, p. 435).
- Boumal, N. (2023). *An introduction to optimization on smooth manifolds*. Cambridge University Press. <https://doi.org/10.1017/9781009166164>
- Casey, C. M., Kartaltepe, J. S., Drakos, N. E., Franco, M., Harish, S., Paquereau, L., Ilbert, O., Rose, C., Cox, I. G., Nightingale, J. W., Robertson, B. E., Silverman, J. D., Koekemoer, A. M., Massey, R., McCracken, H. J., Rhodes, J., Akins, H. B., Amvrosiadis, A., Arango-Toro, R. C., ... Zavala, J. A. (2023). *COSMOS-web: An overview of the JWST cosmic origins survey*. <https://arxiv.org/abs/2211.07865>
- Flaugher, B., Diehl, H. T., Honscheid, K., Abbott, T. M. C., & others. (2015). The dark energy camera. *AJ*, *150*, 150. <https://doi.org/10.1088/0004-6256/150/5/150>
- Innes, M. (2018). Flux: Elegant machine learning with julia. *Journal of Open Source Software*. <https://doi.org/10.21105/joss.00602>
- Jarvis, M., Bernstein, G. M., Amon, A., Davis, C., Lé get, P. F., Bechtol, K., Harrison, I., Gatti, M., Roodman, A., Chang, C., Chen, R., Choi, A., Desai, S., Drlica-Wagner, A., Gruen, D., Gruendl, R. A., Hernandez, A., MacCrann, N., Meyers, J., ... and, R. D. W. (2020). Dark energy survey year 3 results: Point spread function modelling. *Monthly Notices of the Royal Astronomical Society*, *501*(1), 1282–1299. <https://doi.org/10.1093/mnras/staa3679>
- McCleary, J. E., Everett, S. W., Shaaban, M. M., Gill, A. S., Vassilakis, G. N., Huff, E. M., Massey, R. J., Benton, S. J., Brown, A. M., Clark, P., & others. (2023). Lensing in the

- 192 blue II: Estimating the sensitivity of stratospheric balloons to weak gravitational lensing.  
193 *arXiv Preprint arXiv:2307.03295*.
- 194 Mogensen, P. K., & Riseth, A. N. (2018). Optim: A mathematical optimization package for  
195 julia. *Journal of Open Source Software*, 3(24), 615. <https://doi.org/10.21105/joss.00615>
- 196 Perrin, M. D., Sivaramakrishnan, A., Lajoie, C.-P., Elliott, E., Pueyo, L., Ravindranath, S., &  
197 Albert, Loic. (2014). Updated point spread function simulations for JWST with WebbPSF.  
198 In Jr. Oschmann Jacobus M., M. Clampin, G. G. Fazio, & H. A. MacEwen (Eds.), *Space*  
199 *telescopes and instrumentation 2014: Optical, infrared, and millimeter wave* (Vol. 9143, p.  
200 91433X). <https://doi.org/10.1117/12.2056689>
- 201 Perrin, M. D., Soummer, R., Elliott, E. M., Lallo, M. D., & Sivaramakrishnan, A. (2012).  
202 Simulating point spread functions for the James Webb Space Telescope with WebbPSF. In  
203 M. C. Clampin, G. G. Fazio, H. A. MacEwen, & Jr. Oschmann Jacobus M. (Eds.), *Space*  
204 *telescopes and instrumentation 2012: Optical, infrared, and millimeter wave* (Vol. 8442, p.  
205 84423D). <https://doi.org/10.1117/12.925230>
- 206 Revels, J., Lubin, M., & Papamarkou, T. (2016). Forward-mode automatic differentiation in  
207 Julia. *arXiv:1607.07892 [Cs.MS]*. <https://arxiv.org/abs/1607.07892>
- 208 Rieke, M. J., Baum, S. A., Beichman, C. A., Crampton, D., Doyon, R., Eisenstein, D., Greene,  
209 T. P., Hodapp, K.-W., Horner, S. D., Johnstone, D., Lesyna, L., Lilly, S., Meyer, M.,  
210 Martin, P., Jr., D. W. M., Rieke, G. H., Roellig, T. L., Stauffer, J., Trauger, J. T., & Young,  
211 E. T. (2003). NGST NIRCcam scientific program and design concept. In J. C. Mather (Ed.),  
212 *IR space telescopes and instruments* (Vol. 4850, pp. 478–485). International Society for  
213 Optics; Photonics; SPIE. <https://doi.org/10.1117/12.489103>
- 214 Rieke, M. J., Kelly, D. M., Misselt, K., Stansberry, J., Boyer, M., Beatty, T., Egami, E., Florian,  
215 M., Greene, T. P., Hainline, K., Leisenring, J., Roellig, T., Schlawin, E., Sun, F., Tinnin,  
216 L., Williams, C. C., Willmer, C. N. A., Wilson, D., Clark, C. R., ... Young, E. T. (2023).  
217 Performance of NIRCcam on JWST in flight. *Publications of the Astronomical Society of*  
218 *the Pacific*, 135(1044), 028001. <https://doi.org/10.1088/1538-3873/acac53>
- 219 Rieke, M. J., Kelly, D., & Horner, S. (2005). Overview of James Webb Space Telescope and  
220 NIRCcam's Role. In J. B. Heaney & L. G. Burriesci (Eds.), *Cryogenic optical systems and*  
221 *instruments XI* (Vol. 5904, pp. 1–8). <https://doi.org/10.1117/12.615554>
- 222 Rosen, D. M., Carlone, L., Bandeira, A. S., & Leonard, J. J. (2019). SE-sync: A certifiably cor-  
223 rect algorithm for synchronization over the special euclidean group. *The International Jour-*  
224 *nal of Robotics Research*, 38(2-3), 95–125. <https://doi.org/10.1177/0278364918784361>
- 225 Rowe, B. (2010). Improving PSF modelling for weak gravitational lensing using new methods  
226 in model selection. *404*(1), 350–366. <https://doi.org/10.1111/j.1365-2966.2010.16277.x>
- 227 Rowe, B., Jarvis, M., Mandelbaum, R., Bernstein, G. M., Bosch, J., Simet, M., Meyers, J.  
228 E., Kacprzak, T., Nakajima, R., Zuntz, J., Miyatake, H., Dietrich, J. P., Armstrong, R.,  
229 Melchior, P., & Gill, M. S. S. (2015). *GalSim: The modular galaxy image simulation*  
230 *toolkit*. <https://arxiv.org/abs/1407.7676>
- 231 Stetson, P. B. (1987). DAOPHOT: A COMPUTER PROGRAM FOR CROWDED-FIELD  
232 STELLAR PHOTOMETRY. *Publications of the Astronomical Society of the Pacific*,  
233 99(613), 191. <https://doi.org/10.1086/131977>